architecture. Minimization of their surface free energy through a balance of adhesion and elastic forces[6] could lead to vesicle distortion and to the honeycomb surface patterns, Fig. 2*c*, *d*. This tentative model is represented in Fig. 3.

Specific control experiments have cast further light on the origin of the observed morphologies and patterns. TEG allows formation of the surface patterns, whereas ethylene glycol and higher-molecular-weight polyethylene glycols do not. Increasing the mole ratio of water, varying the mole ratio of surfactant or changing the temperature, allow formation of a mesolamellar aluminophosphate, but devoid of surface patterning. A small-molecule amine unable to form self-assembled aggregates results in normal faceted crystal habits of one-dimensional (chain), two-dimensional (porous sheet) and three-dimensional (open-framework) aluminophosphate materials[11]. These experiments emphasize the synergistic role of the surfactant-co-surfactant templates in determining morphology and surface patterning in the MLA synthesis system.

Our model for pattern formation is akin to some of those proposed in the biomineralization literature for the creation of exoskeletons[12,13]. One prevailing idea is that radiolaria skeletons grow by the secretion of silica into a network of bubble-like alveoli[12–16]. This model has features in common with our growing aluminophosphate sphere covered by vesicles. The concentric nature of the vesicles could facilitate the deposition of replica features on the surface of the bowls. This could account for the concentric ring and platelet formations in the bowls of Fig. 2*c*.

It is interesting to compare the morphologies and patterns of the artificial inorganic assemblies (Fig. 2*c*, *d*) with those of the siliceous skeletons of diatoms and radiolaria (Fig. 4*a*, *b*).[14–16] The skeletal features are of similar size and form to those of the surfactant-based aluminophosphate morphologies. Examples of surface bowl-like features akin to the synthetic ones in Fig. 2*b* are common in radiolaria, Fig. 4*c*. Another common feature is the lack of long-range order in the aluminophosphate regions of the synthetic ultrastructures, a situation similar to [illegible] amorphous silica protozoan exoskeletons of radiolaria a[nd] diatoms[17], as well as the amorphous walls of micelle-templa[ted] mesoporous silicas[1–3].

It would seem that there are interesting parallels to be dra[wn] between protozoan diatoms and radiolaria and our artifi[cial] inorganic assemblies. The inorganic materials reported here [are] hierarchical and display structural features on length scales ra[nging] ing from submicrometre to millimetres. The ability to synth[esize] ically control macroscopic form and surface patterns [of] inorganic materials could find important application in ar[eas] such as catalysis, separation technology and the development [of] new functional materials[18].

Received 15 May; accepted 12 October 1995.

1. Kresge, C. T. *et al. Nature* **359**, 710–712 (1992).
2. Beck, J. S. *et al. J. Am. chem. Soc.* **114**, 10834–10843 (1992).
3. Monnier, A. *et al. Science* **261**, 1299–1303 (1993).
4. Kaler, E. W. & Martino, A. *Langmuir* **11**, 779–784 (1995).
5. Thomas, B. N., Safinya, C. R., Plano, R. J. & Clark, N. A. *Science* **267**, 1635–1638 (19[95])
6. Israelachvili, J. N. *Intermolecular and Surface Forces* 2nd edn (Academic, New York, 19[92])
7. Hoffmann, H. *Adv. Mater.* **6**, 116–129 (1994).
8. Haslop, W. P., Allonby, J. M., Akred, B. J. & Messenger, E. T. US Patent No. 4,618,[671] (1986).
9. Akred, B. J., Messenger, E. T. & Nicholson, W. J. US Patent no. 4,659,497 (1987).
10. Fendler, J. H., *Membrane Mimetic Chemistry* (Wiley, New York, 1982).
11. Oliver, S. *et al. Stud. Surf. Sci. Catal.* **84**, 219–225 (1994).
12. Simkiss, K. & Wilbur, K. M. *Biomineralization: Cell Biology and Mineral Deposi[tion]* (Academic, San Diego, 1989).
13. Mann, S., Webb, J. & Williams, R. (eds) *Biomineralization: Chemical and Biochemical Per[spectives]* (VCH, New York, 1989).
14. Takahashi, K. (ed) *Radiolaria* (Ocean Biocoenosis Ser. no. 3, Woods Hole Oceanogra[phic] Institution, Woods Hole, MA, 1991).
15. Richard, M. (ed.) *Ouvrage Dedie a la Memoire du Professor Henry Germain* (Koeltz Scien[tific] Konigstein, 1990).
16. Anderson, O. R. *Radiolaria* (Springer, New York, 1983).
17. Mann, S. *J. mater. Chem.* **5**, 935–946 (1995).
18. Oliver S. & Ozin, G. A. *Adv. Mater.* (In the press).

SUPPLEMENTARY INFORMATION. Crystallographic refinement data are available on requ[est]. Contact Mary Sheehan at the London editorial office of *Nature*.

ACKNOWLEDGEMENTS. This work was supported by the Natural Sciences and Engineer[ing] Research Council of Canada. S.O. was supported in part by the Ontario Graduate Scholar[ship] program.

High concentrations and photochemical fate of oxygenated hydrocarbons in the global troposphere

Hanwant B. Singh*, M. Kanakidou†, P. J. Crutzen‡ & D. J. Jacob§

* NASA Ames Research Center, Moffett Field, California 94035, USA
† Centre des Faibles Radioactivites, CNRS-CEA, F-91198 Gif-sur-Yvette Cedex, France
‡ Max Planck Institute for Chemistry, D-55020 Mainz, Germany
§ Harvard University, Cambridge, Massachusetts 02138, USA

OXYGENATED species in the atmosphere are important sources of free radicals and are intricately linked with the fate of nitrogen oxides (NO_x), which are themselves necessary for tropospheric ozone formation[1,2]. With the exception of formaldehyde, oxygenated hydrocarbons have rarely been measured in the free troposphere. Here we report airborne measurements indicating the presence of high concentrations (compared to those of routinely measured C_2–C_6 tropospheric hydrocarbons[3,4]) of acetone and methanol. We use a three-dimensional model to show that acetone photochemistry provides a quantitatively significant (up to 50%) pathway for sequestering NO_x in the form of peroxyacetylnitrate, a relatively unreactive temporary reservoir of NO_x. Furthermore, in the dry regions of the upper troposphere, acetone can provide a large primary source of HO_x ($OH + HO_2$) radicals, resulting in increased ozone production. This surprisingly significant contribution of such oxygenated hydrocarbons to tropospheric NO_x, HO[x] and ozone cycling is likely to be affected by their changing natural and anthropogenic emissions due to land-use change, biomass burning and alcohol-based biofuel use.

Limited measurements of alcohols and carbonyls have been reported from ground sites generally in rural/urban environments[5–7]. Recently, we have developed and tested a semi-automated airborne instrument that uses a Reduction Gas Detector (RGD) for the sensitive (~10 parts per trillion (10^{-12} by volume, p.p.t.) detection of carbonyls in real time[8,9]. We have now expanded this to include alcohols. Figure 1 shows a chromatogram that demonstrates the separation and detection of acetaldehyde, acetone, methanol and ethanol from free tropospheric air. A parallel instrument also measured peroxyacetyl nitrate (PAN) to a sensitivity of ~1 p.p.t. Data were collected in February–March 1994 during the NASA Pacific Exploratory Mission, PEM-West (B); an airborne campaign to study the atmosphere over the Pacific Ocean.

Figure 2 shows the latitudinal distribution of acetone and PAN in the free troposphere (5–10 km height) based on a series of six flights over the Pacific Ocean starting from 40° N to 10° S over a longitude of 125° W to 140° E. During these selected missions, westerly air flows and the great distance from the Asian continent precluded a direct effect of continental emissions, and these air samples should represent near-background conditions for this season. In the free troposphere, acetone concentrations of the order of 500 p.p.t. were present at northern mid-latitudes and declined to ~200 p.p.t. at southern latitudes. These mixing ratios are similar to those measured in the Canadian Arctic and subarctic when clean conditions prevailed[9], but are higher than

reported by Arnold *et al.*[10] for the mid-latitude tropo-
re (44° N; February–May) over Europe using an indirect
od involving chemical ionization mass spectrometry. PAN
entrations in the vicinity of 100 p.p.t. were present in the
hern free troposphere, although its abundance was highly
able. Near the tropics, mixing ratios below 10 p.p.t. were
seen. PAN exhibited a strong vertical gradient, and its
entrations in the marine boundary layer were typically
p.t. Acetaldehyde could not be rigorously quantified
use of difficulties involving its calibration. Based on relative
onse factors determined in the laboratory, it would seem
30–100 p.p.t. of acetaldehyde were nearly always present.
the free troposphere ~700 p.p.t. of methanol were present
orthern mid-latitudes, declining to ~400 p.p.t. at southern
udes (Fig. 3). In general, ethanol abundance was an order
agnitude lower than that of methanol. There were instances
ethanol was below the detection limit of 10 p.p.t. No latitu-
profiles for alcohols or acetone have been reported in the

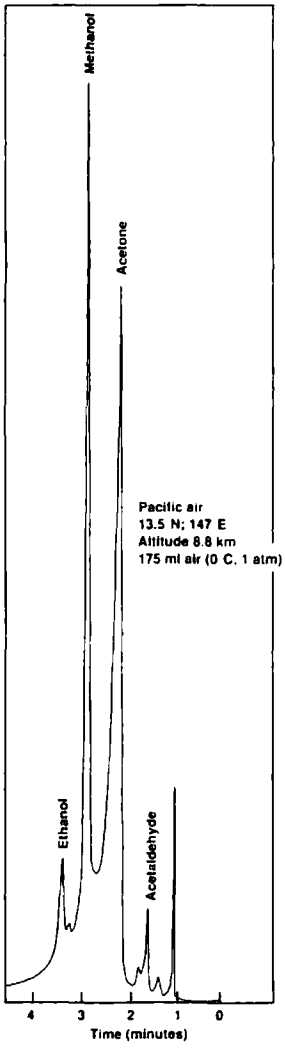

1 Chromatogram showing the detection and separation of selected
enated species from free tropospheric air. A 175-ml sample of air
eeze trapped at −140 °C in a sample loop, and its constituents
rated on a 30-m stripper (for water removal) and a 60-m analytical
rtz capillary column (0.53 mm i.d., 1 μm DB wax film coating; 80 °C)
detected with a Reduction Gas Detector (RGD). A heated (20 °C)
on probe is used for sampling, and all calibrations, using permeation
es held at 0 °C, are done in-flight in a manner that mimics ambient
sampling. The tailing of the acetone peak is probably due to its slow
ase from the mercuric oxide bed in the RGD.

literature for comparison. Limited measurements were also made in the mid-latitude lower stratosphere (331±104 p.p.b (10^{-9} by volume) O_3; −55 to −69 °C dew point). Under these conditions, mixing ratios of acetone and methanol were 148±63 p.p.t. and 95±51 p.p.t. respectively, while ethanol was generally below the detection level.

The main removal process for acetone, methanol and ethanol is expected to be reaction with OH radicals and photolysis (important for acetone only). Based on published OH radical rate coefficients[11], the best estimates for OH radical abundance (10^6 molecules per cm^3; methyl chloroform lifetime of 5.0 yr), and known photolytic cross-sections, we estimate that average lifetimes of acetone, methanol and ethanol are of the order of 16 days, 16 days and 4 days, respectively. To balance the measured abundances and the removal rates, a global source of about 50 Tg yr^{-1} acetone, 45 Tg yr^{-1} methanol and 15 Tg yr^{-1} ethanol is required. Although these species are miscible with water, their Henry's Law coefficients are relatively low (at 25 °C: 32 M atm^{-1} for acetone; 220 M atm^{-1} for alcohols) and removal by washout/rainout processes or the oceanic sink should not compete favourably with removal by reaction with OH radicals and photolysis[12]. Upper-tropospheric cloud systems may take in some alcohols, but are likely to desorb them during precipitation. The north–south latitudinal gradient implies larger sources in the north, but we note that photochemical removal at this time of the year (February) is about 1.5–2 times higher in the Southern Hemisphere than the Northern Hemisphere. Additional gradients between the marine and continental environments may also exist.

Alcohols on further oxidation form photochemically active carbonyls and free radicals[13].

$$CH_3OH + OH + (O_2) \rightarrow CH_2O + HO_2 + H_2O$$
$$C_2H_5OH + OH + (O_2) \rightarrow CH_3CHO + HO_2 + H_2O$$

Acetone also can easily react with OH radical and be photolysed to produce free radicals (for example, HO_2) and several stable species such as PAN, and acetic and peracetic acids[9,14].

$$CH_3COCH_3 + h\nu + (2O_2) \rightarrow CH_3COO_2 + CH_3O_2$$
$$CH_3COO_2 + NO_2 \leftrightarrow CH_3COO_2NO_2\,(PAN)$$
$$CH_3COO_2 + HO_2 \rightarrow CH_3COOH + O_3\ (67\%)$$
$$\rightarrow CH_3COO_2H + O_2\ (33\%)$$
$$CH_3COO_2 + NO + (O_2) \rightarrow CH_3O_2 + CO_2 + NO_2$$
$$CH_3O_2 + NO \rightarrow CH_3O + NO_2$$
$$CH_3O + O_2 \rightarrow CH_2O + HO_2$$
$$CH_2O + h\nu \rightarrow CO + H_2\ (\sim 50\%)$$
$$\rightarrow H + CHO + (2O_2)$$
$$\rightarrow 2HO_2 + CO\ (\sim 30\%)$$
$$CH_2O + OH \rightarrow CHO + H_2O\ (\sim 20\%)$$

We have studied the role of acetone in PAN formation by incorporating detailed acetone and C_1–C_3 hydrocarbon chemistry in a three-dimensional model of the atmosphere[14]. Based on the inventory suggested by Singh *et al.*[9], a 49 Tg yr^{-1} global source of acetone was incorporated in this model. Emissions from vegetation were scaled to the annual mean net primary productivity, while anthropogenic emissions were distributed in a manner similar to those of CO_2. This resulted in acetone concentrations shown in Fig. 4*a*. Model PAN concentrations were calculated with and without the inclusion of acetone. Figure 4*b* shows the PAN mixing ratios that could be attributed exclusively to acetone chemistry. It is evident that acetone is responsible for sizeable (10–45 p.p.t.) concentrations of PAN in the free troposphere. Its effect is greatest in the middle and upper troposphere where photolysis of acetone is quite efficient and PAN is

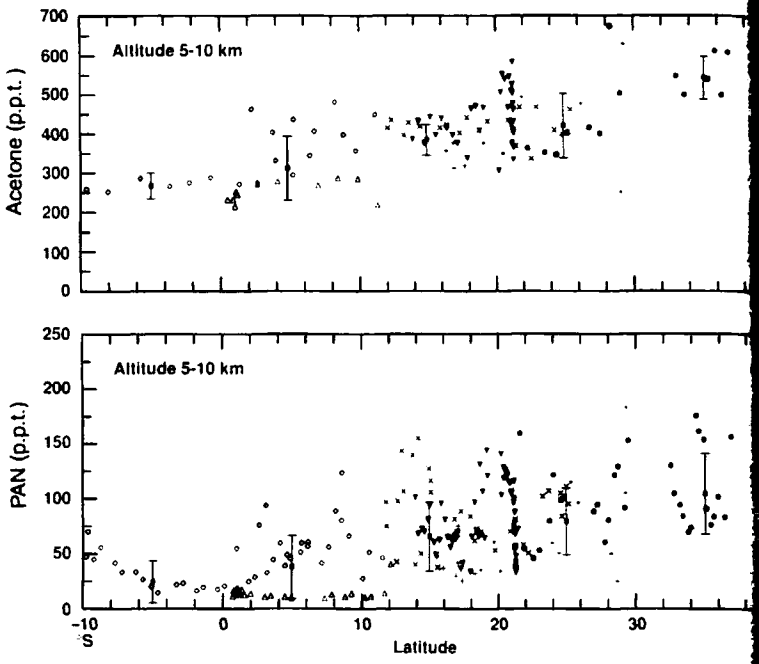

FIG. 2 Latitudinal distribution of acetone (top panel) and PAN (bottom panel) in the free troposphere over the Pacific. These data are for 5–10 km altitude, and are based on a series of six aircraft flights performed during 7–19 February, 1994. Each flight is represented by a separate symbol. Transit flights started from California (38° N) to Hawaii (21° N) (filled circles) and Hawaii to Guam (13° N) (inverted filled triangles). Four additional flights were undertaken north (+ and x) and south (○, △) from Guam. Each filled square and the line extending from it shows mean±1 standard deviation for data within the 10° latitude belt.

most stable. Based on model results and comparison with data, up to 50% of observed PAN may be formed by this mechanism. Model results also show that acetone photolysis can produce 10^5–10^6 molecules per cm^3 of peroxyacetyl radicals with highest values in the tropics. We suggest that acetone provides an important pathway in storing NO_x in the form of PAN, and must be included in global models that aim to accurately simulate ozone in the troposphere.

We also find that acetone is an important and previously unrecognized source of HO_x radicals in the upper troposphere. Current photochemical models identify the two main upper-tropospheric sources of HO_x as the reaction of $O(^1D)$ with water vapour ($O_3 + h\nu \rightarrow O(^1D) + O_2$; $O(^1D) + H_2O \rightarrow 2OH$) and the photolysis of CH_2O. The main source of CH_2O in these models is the oxidation of methane by OH radicals; therefore one must view the $O(^1D) + H_2O$ reaction as the primary source of HO_x and CH_2O as an amplifier of this source. Under dry condit of the upper troposphere, where the reaction $O(^1D) + H_2$ relatively slow, acetone makes an important additional contr tion to the primary source of HO_x. The photolysis of ace here yields two HO_2 and two CH_2O molecules ($NO \gg HO_2$), 30% of the CH_2O molecules photolyse via the radical branc yield two more HO_2 molecules. Thus the HO_x yield from photolysis of acetone is ~3.2 ($2 + 4 \times 0.30$), as compared t yield of 2 from the reaction of $O(^1D) + H_2O$. In a simple ph chemical model calculation for the upper troposphere at equinox (40° N, 11 km, 50 p.p.b. O_3, 90 p.p.m. (10^{-6} by volu H_2O and 0.5 p.p.b. acetone), we find 24-hour average HO_x p duction rates of 7×10^3 molecules per cm^3 per s from reac of $O(^1D) + H_2O$ and 9×10^3 molecules per cm^3 per s from ph lysis of acetone. When all primary and secondary sources included, acetone may enhance total HO_x concentrations by

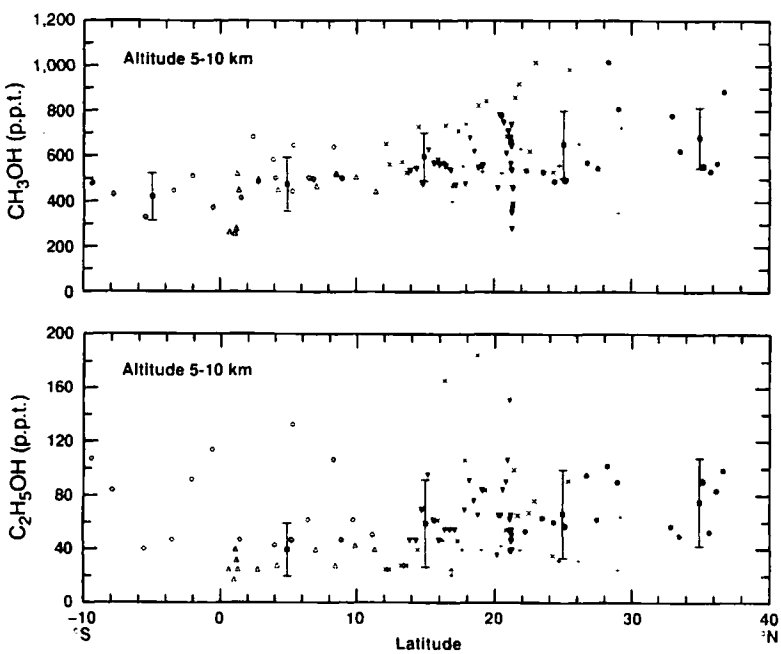

FIG. 3 Latitudinal distribution of methanol (top pa and ethanol (bottom panel) in the free troposphere the Pacific Ocean. Symbols are as in Fig. 2.

FIG. 4 Three nd PAN forn 49 Tg yr^{-1} esults are fc he central P

o 30% in tl critically c $HO_2 \rightarrow NO_2$ roposphere may have a assessing th onic aircra sphere sugg by O_3 photc Although ot emitted ot been sul ions from have been rarely been o those of i species[18]. In rn United tone, metha 6.0 p.p.b. ar input inferre methyl bute from vegeta reported[19]. T formed fron within th $C_5H_{10}O \leftrightarrow (C$ $H_2O \leftrightarrow C_2H_5$ common pre Anthropo trations of areas[6]. In c (China/Hon Molar ratios ΔCO) were and 0.0004 f genic emissic yr^{-1} acetone There is littl these species smouldering was identifie CO of 0.025. ted at 200 T yr^{-1} is possil

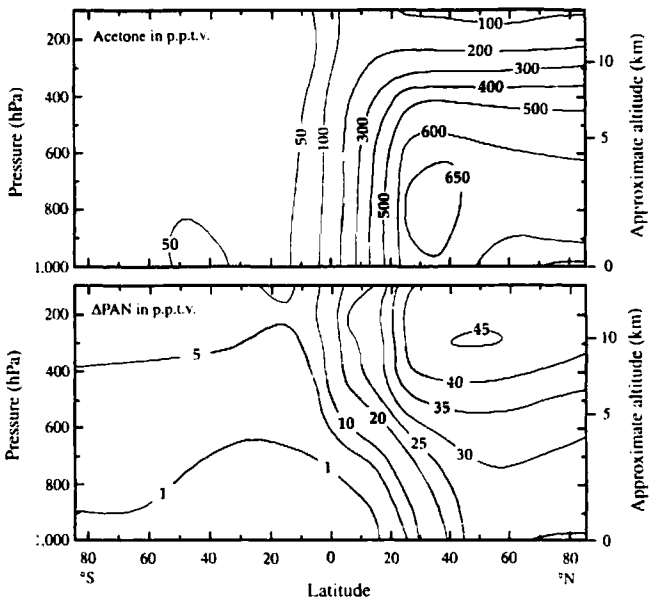

Three-dimensional model results showing acetone distribution, AN formation from acetone chemistry. *a*, Acetone distribution with g yr^{-1} total source; *b*, PAN due to acetone chemistry alone. Model s are for 1 March and show a height–latitude cross-section over ntral Pacific (175° E longitude).

% in the mid-latitude upper troposphere. As HO_x radicals ally control the production of O_3 via the $NO + \rightarrow NO_2 + OH$ reaction, the presence of acetone in the upper osphere enhances the production of O_3. This enhancement have a number of important implications, in particular for sing the atmospheric effects of NO_x emissions from sub- aircraft. Recent HO_x measurements in the lower strato- e suggest that HO_x sources in addition to those predicted photolysis are required to explain the observations[15]. though PAN is a purely photochemical product which is mitted directly, sources of oxygenated hydrocarbons have een subject to rigorous studies. In studies of biogenic emis- from plants, acetone, acetaldehyde, methanol and ethanol been frequently detected although their emissions have been quantified[16,17]. Emissions of methanol comparable ose of isoprene have been reported from a variety of plant es[18]. In a field study at a forested rural site in the southeast- United States, average mixing ratios of acetaldehyde, ace- methanol and ethanol of respectively 0.8 p.p.b., 3.3 p.p.b., .p.b. and 1.0 p.p.b. were measured, and a strong biogenic t inferred[7]. Emission of copious quantities of highly reactive yl butenol {C-C(C)(OH)-C=C or $C_5H_{10}O$}, a C_5 alcohol, vegetation at a forested site in Colorado has also been rted[19]. The possibilities that carbonyls and alcohols may be ed from reaction of known biogenic chemicals and water in the plant enzyme system ($C_5H_8 + H_2O \leftrightarrow$ $_{10}O \leftrightarrow (CH_3)_2CO + C_2H_4$; $C_2H_4 + 2H_2O \leftrightarrow 2CH_3OH$; $C_2H_4 +$ $\leftrightarrow C_2H_5OH$), and that many of these chemicals may have mon precursors, should be explored.

nthropogenic emissions are also evident from high concen- ons of oxygenates that have been reported from polluted s[6]. In our airborne study, a plume of Asian emissions na (Hong Kong) was intersected over the western Pacific. ar ratios of enhancement of species X relative to CO ($\Delta X/$) were found to be 0.003 for acetone, 0.007 for methanol 0.0004 for ethanol. Scaling to a total global CO anthropo- c emission[20] of 445 Tg yr^{-1} implies a source of about 2.7 Tg acetone, 3.8 Tg yr^{-1} methanol and 0.4 Tg yr^{-1} ethanol. re is little doubt that biomass burning is also a source for e species. In a laboratory study[21] designed to simulate the uldering combustion of ponderosa pine sapwood, methanol identified as a product with a molar ratio with respect to of 0.025. With global CO biomass burning emissions estima- at 200 Tg yr^{-1} (ref. 20), a methanol source of about 6 Tg is possible. We have earlier reported that biomass burning emissions of acetone may be in the vicinity of 10 Tg yr^{-1} (ref. 9).

Oxygenated species are also known to be intermediate products of hydrocarbon oxidation, with methane as the most important source for methanol ($2CH_3O_2 \rightarrow CH_3OH + CH_2O + O_2$) and propane for acetone[2,22]. We have attempted to simulate these reactions in our model, after Madronich and Calvert[14,23]. Assuming removal of methanol by OH oxidation, and by rainout/washout and deposition (0.1 cm s^{-1}) processes, our model calculations (for 1 March) suggest that ~160 p.p.t. (global average) of methanol could be synthesized from these reactions, and these mixing ratios may approach 500 p.p.t. in the tropical lower troposphere. Similarly, 100–300 p.p.t. of acetone and 1–10 p.p.t. of ethanol could be synthesized in the middle troposphere via these oxidation mechanisms alone[9,14,22].

Yet another source may be found in the oceans. Evidence for supersaturation of some carbonyls in sea water has been published, but the data are sparse and inconclusive[24]. Oceans are known to be supersaturated with methyl halides[25]. A possible source for methanol in sea water is from the hydrolysis of methyl halides ($CH_3X + H_2O \rightarrow CH_3OH + HX$) which takes place at a relatively slow rate[26]. Suffice it to say that substantial anthropogenic and natural sources of these (and other) oxygenated species are present but remain to be rigorously studied and quantified.

In recent years ethanol has been added to gasoline to achieve cleaner combustion, and the use of ethanol and methanol as biofuels is likely to increase in the future. Measurements of these species in the atmosphere have received attention only recently, in large part because these vapours are difficult to measure, are poorly retained by solid sorbents, and can be easily lost in canisters which are often used as a means of sample collection and storage. Here we have shown that these oxygenated species are globally ubiquitous, can participate in photochemistry of the troposphere in an important way, and have complex biogenic (as well as man-made) sources which require better quantification and further study. It is likely that other oxygenated species are present but have not yet been identified. □

Received 21 April; accepted 19 September 1995.

1. Lloyd, A. C. *NBS spec. publ.* **557**, 27–48 (1979).
2. Singh, H., B. & Hanst, P. L. *Geophys. Res. Lett.* **8**, 941–944 (1981).
3. Singh, H. B. & Zimmerman, P. B. *Adv. envir. Sci. Technol.* **24**, 177–235 (1992).
4. Blake, D. R. et al. J. geophys. Res. **99**, 1699–1719 (1994).
5. Cavanagh, L., Schadt, C. & Robinson, E. *Envir. Sci. Technol.* **3**, 251–257 (1969).
6. Snider, J. R. & Dawson, G. A. *J. geophys. Res.* **90**, 3797–3805 (1985).
7. Goldan, P. D., Kuster, W. C., Fehsenfeld, F. C. & Montzka, S. A. *J. geophys. Res.* (in the press).
8. O'Hara, D. & Singh, H. B. *Atmos. Envir.* **22**, 2613–2615 (1988).

9. Singh, H. B. *et al. J. geophys. Res.* **99**, 1805–1819 (1994).
10. Arnold, F., Knop, G. & Zeiereis, H. *Nature* **321**, 505–507 (1986).
11. DeMore, W. B. *et al. Chemical Kinetics and Photochemical Data for Use in Stratospheric Modeling* (JPL Publ. No. 94-26, Jet Propulsion Laboratory, Pasadena, CA, 1994).
12. Betterton, E. A. *Adv. envir. Sci. Technol.* **24**, 1–50 (1992).
13. Atkinson, R. *Atmos. Envir.* **24A**, 1–41 (1990).
14. Kanakidou, M. & Crutzen, P. J. *Chemosphere* **26**, 787–801 (1993).
15. Wennberg, P. *et al. Science* **266**, 398–404 (1994).
16. Isidorov, V. A., Zenkench, I. G. & Iofe, B. V. *Atmos. Envir.* **19**, 1–8 (1985).
17. Isidorov, V. A. *Organic Chemistry of the Earth's Atmosphere* (Springer, Berlin, 1990).
18. MacDonald, R. C. & Fall, R. *Atmos. Envir.* **27A**, 1709–1713 (1993).
19. Goldan, P. D., Kuster, W. C., Fehsenfeld, F. C. & Montzka, S. A. *Geophys. Res. Lett.* **20**, 1039–1042 (1993).
20. Lobert, J. M. *et al.* in *Global Biomass Burning* (ed. Levine, J. S.) 289–304 (MIT, Cambridge, MA, 1991).
21. McKenzie, L. M., Hao, W. M., Richards, G. N. & Ward, D. E. *Atmos. Envir.* **28**, 3285 (1994).
22. Kanakidou, M., Singh, H. B., Valentin, K. M. & Crutzen, P. J. *J. geophys. Res.* **96**, 15413 (1991).
23. Madronich, S. & Calvert, J. G. *J. geophys. Res.* **95**, 5697–5715 (1990).
24. Zhou, X. & Mopper, K. *Envir. Sci. Technol.* **24**, 1864–1869 (1990).
25. Singh, H. B., Salas, L. J. & Stiles, R. E. *J. geophys. Res.* **88**, 3684–3690 (1983).
26. Elliott, S. & Rowland, F. S. *J. atmos. Chem.* **20**, 229–236 (1995).

ACKNOWLEDGEMENTS. We thank all PEM-West (B) participants for their support. Sugg... by A. R. Ravishankara of the NOAA Aeronomy Lab were appreciated. This work was su... by the NASA Global Tropospheric Experiment, CNRS and CEA.

Experimental evidence for the origin of lead enrichment in convergent-margin magmas

James M. Brenan*, Henry F. Shaw* & Frederick J. Ryerson*†

* Earth Sciences Division, † Institute for Geophysics and Planetary Physics, Lawrence Livermore National Laboratory, PO Box 808, L-202, Livermore, California 94551, USA

It has been proposed[1–5] that the low Ce/Pb ratio of subduction-related basalts, relative to their oceanic counterparts, arises by the preferential transfer of lead to the mantle wedge (overlying the subducting slab) by non-magmatic processes. Fluxing of the mantle wedge by low-Ce/Pb fluids, generated by the dehydration of subducted oceanic crust, is one mechanism favoured for this process (see, for example, ref. 5). Here we report the results of a series of high-pressure experiments, which confirm that low-Ce/Pb fluids coexist with the dominant mineral phases (garnet and clinopyroxene) produced during high-pressure dehydration of altered basalt. Our results show that the production of subduction-zone magmas from mantle sources fluxed by basalt-derived fluid is a mechanism by which relatively lead-rich, cerium-poor, mantle-derived material is added to the continents. The lead enrichment of the Earth's continental crust is thus a continuing process occurring at convergent margins.

The Ce/Pb ratio in island-arc basalts (~3) is similar to that of average continental crust, but considerably below that of oceanic basalts (~25) and the bulk Earth (~10; summarized in ref. 5). Owing to similar bulk solid/liquid partition coefficients, these elements are not significantly fractionated during mantle melting processes, and melt compositions reflect the approximate Ce/Pb ratio of their source regions[1]. The above-described differences, together with the general similarity between the Ce abundances of island-arc basalts (IABs) and oceanic basalts, suggest that the source regions for IABs are enriched in Pb relative to oceanic mantle. As subduction-related magmatism is a con... ing process that adds low-Ce/Pb material to the contin... knowledge of the mechanism(s) of Pb-enrichment in IABs provide insight into both the origin of Pb-enrichment in continental crust, and the complementary depletion of thi... ment in the oceanic mantle.

Recently, Miller *et al.*[5] showed that Pb from two isotopi... distinct sources is present in the IABs erupted on Unmak ... in the Aleutian archipelago. One source, with high $^{207}Pb/^{204}Pb$ and low Ce/Pb, is consistent with pelagic sediment. The ... source, despite having low and mantle-like $^{207}Pb/^{204}Pb$, ha... tinctly non-mantle Ce/Pb (that is, <5 compared to ~25 fo... oceanic mantle). Miller *et al.* hypothesized that a low-C... mantle component could be produced by the preferential ex... tion of Pb from subducted oceanic crust by a fluid phase. T... fer of Pb from subducted oceanic crust to arc magmas by... process constitutes a means to explain the origin of the co... mentary nature of the Ce/Pb ratios of continental crust ... oceanic mantle. To test this hypothesis, we have condu... piston-cylinder experiments at 2.0 GPa and 900 °C to deter... the Ce/Pb ratio of fluids coexisting with phases that ma... residual during high-pressure basalt dehydration, namely ... pyroxene and garnet.

Garnet/fluid and clinopyroxene/fluid partition coefficient... Pb, Ce, Nd, Sm and Yb were measured in experiments ... consisted of loading known quantities of trace-element do... (dried nitrate solutions) with garnet or clinopyroxene and ... ($H_2O \pm NaCl$) + excess SiO_2 + albite (~3 wt%) in welded Pt ... sules. Samples were equilibrated in the piston cylinder for ... days, during which time the garnet and clinopyroxene recry... lized; the inclusion of SiO_2 and albite along with the inh... solubility of clinopyroxene and garnet produced a rea... 'eclogite-fluid' composition[6]. After an experiment, capsules ... cleaned in concentrated nitric acid, then pierced in ultra-... distilled water. Newly-formed crystals (pyrope-rich garnet, ... diopsidic clinopyroxene; see ref. 6) were typically greater ... 300 μm in size and were easily removed by hand-picking. ... post-experiment fluid, including quenched solids ('fish ...

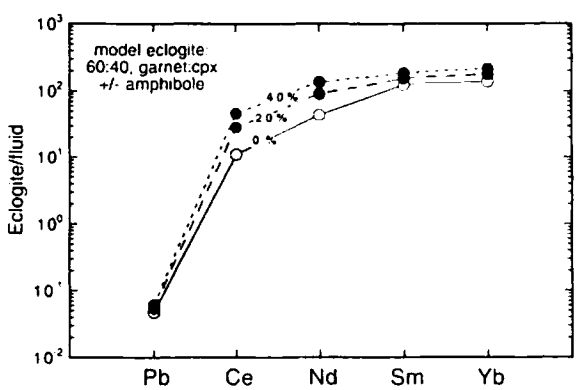

FIG. 1 Bulk eclogite/aqueous fluid partition coefficients for the ... and Pb. Bulk partition coefficients were calculated using the ave... clinopyroxene and garnet/aqueous fluid values measured in the ... and assuming a model eclogite mode (wt% of each mineral in ... mixture) of 60:40; garnet:clinopyroxene. Clinopyroxene/aqueous ... partition coefficients for Ce were determined from the relation $D_{Ce} = 0.3D_{Nd}$ (ref. 11) and are consistent with the Ce content of run-pr... crystals and mass balance (see text). The effect of adding amph... (20 and 40%) to the residue (as a model for incomplete dehydra... was assessed by calculating amphibole/aqueous fluid par... coefficients assuming values of D_{REE} amphibole/clinopyroxene o... (Ce), 3.1 (Nd), 1.9 (Sm) and 2.5 (Yb), as obtained from mineral/... partitioning experiments[11,19]. The amphibole/aqueous fluid par... coefficient for Pb is from ref. 6. Note that the calculated bulk par... coefficients for the REE are more than 200 times larger than fo... and this effect is expected to be largest during the onset of dehydr... (when the amphibole mode is high).